CHAPTER II

THEORETICAL BACKGROUND AND LITERATURE REVIEW

2.1 Carbon dioxide emission

Human activities result in the generation of greenhouse gases (GHGs) into the atmosphere. The greenhouse gases are composed mainly of carbon dioxide (CO_2), methane (CH_4), chlorofluorocarbons (CFCs), and nitrous oxide (N_2O), which are contributing to the global warming phenomena considerably (Kaithwas et al., 2012). Among these gases, the contribution of CO_2 emission is assumed to cause the greatest impact to the green house effect accounting for approximately 55% of the observed global warming. It is estimated that the future global CO_2 emissions will increase from approximately 7.4 GtC (billion tons of atmospheric carbon)/year in 1997 to approximately 26 GtC/year in 2100 (Mercedes et al., 2004). Several suggestions had been made in order to reduce CO_2 emissions into the atmosphere, which are reducing energy consumption by increasing the efficiency of energy conversion, switching to less carbon intense fuels and using renewable energies. Precisely, these options may not be efficient to mitigate global warming in future, so the development in the technology of CO_2 capture and storage provides a mid-term solution to mitigate the environmental impact.

2.2 Carbon dioxide capture technology

Generally, carbon dioxide is often caused by the use of burning fossil fuel (including coal, natural gas and oil) from industrial and human activities. The technology of CO_2 capture and storage in fossil fuel power plants nowadays can be categorized into three basic routes, namely, pre-combustion capture, oxy-fuel combustion capture and post-combustion capture.

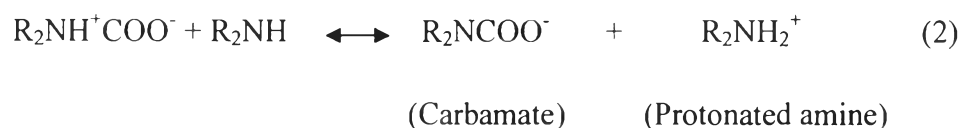## 2.3 Reviews of possible CO_2 separation techniques

In post combustion capture, CO_2 is removed from the flue gas after combustion. It is the most practical approach as it can be retrofitted into the existing process without much modification of the existing plants. The processes mainly involve

chemical absorption process, physical adsorption process, membrane and cryogenic separation. Chemical absorption and physical adsorption gain more focus because cryogenic separation requires high energy, while most membrane separation methods are still at their development stage (Oh TH, 2010).

2.3.1 Alkanolamine absorption technology

Alkanolamines have been found to effectively capture CO_2 from gas stream. They have been extensively used for decades in gas-treating unit. One of the advantages of alkanolamines is that, structurally, they contain at least one hydroxyl group, which helps to reduce vapor pressure and also to increase their solubilities in aqueous solution (Kohl and Reisenfeld, 1985). The amino group provides sufficient alkalinity to absorb CO_2. Alkanolamines can be categorized into three classes: primary, secondary, and tertiary amines. The classification is based on the numbers of substituting groups attached to the nitrogen atom of the molecule. Table 2.1 shows common primary amines, e.g. monoethanolamine (MEA) and diglycolamine (DGA); secondary amines, e.g. diethanolamine (DEA) and diisopropanolamine (DIPA); and tertiary amines, e.g. triethanolamine (TEA) and methyldiethanolamine (MDEA).

Typically, primary and secondary amines react to form a carbamate species, and the reaction may or may not proceed through an intermediate called the zwitterions.

$$CO_2 + R_2NH \longleftrightarrow R_2NH^+COO^- \quad \text{(Zwitterions)} \quad (1)$$

$$R_2NH^+COO^- + R_2NH \longleftrightarrow R_2NCOO^- + R_2NH_2^+ \quad (2)$$

$$\text{(Carbamate)} \quad \text{(Protonated amine)}$$

Tertiary amines cannot form a carbamate species, because they do not have hydrogen attached to the nitrogen atom. Typically, the tertiary amines react according to equation (3).

$$CO_2 + R_3N + H_2O \longleftrightarrow HCO_3^- + R_3NH^+ \quad (3)$$

$$\text{(Bicarbonate)}$$
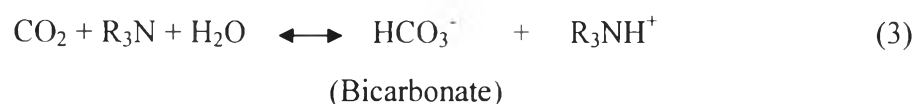
As described by Kohl and Nielsen (1997), primary and secondary amines usually react faster than tertiary amines, and CO_2 has higher heats of absorption in these amines. Heats of reaction at 15 °C and unloaded conditions are approximately 20.3 and 14.8 kcal/mole for MEA and MDEA, respectively. Among many amines, MEA is the most widely used because MEA has the highest alkalinity; hence, it reacts most rapidly with CO_2. As well, it can be reclaimed with ease from the contaminated solution. In general, MEA has the highest CO_2 separation rate, which should lead to relatively low overall costs. However, MEA requires a large amount of energy for regeneration, degrades most rapidly in the presence of oxygen (O_2), has the highest corrosivity among commercial amines, and has a substantially higher vapor pressure than other alkanolamines, resulting in significant vaporization and solvent losses. At different operating conditions being tested and proven with a particular amine, they become accepted on an industry-wide basis. Thus, each amine has a currently "accepted" range of process conditions and parameters associated with it. These "accepted" conditions and parameters are discussed below. Some of the typical operating conditions for common amines are summarized in Table 2.2.

Table 2.1 Structural formula of common alkanolamines (Kohl and Reisenfeld, 1985)
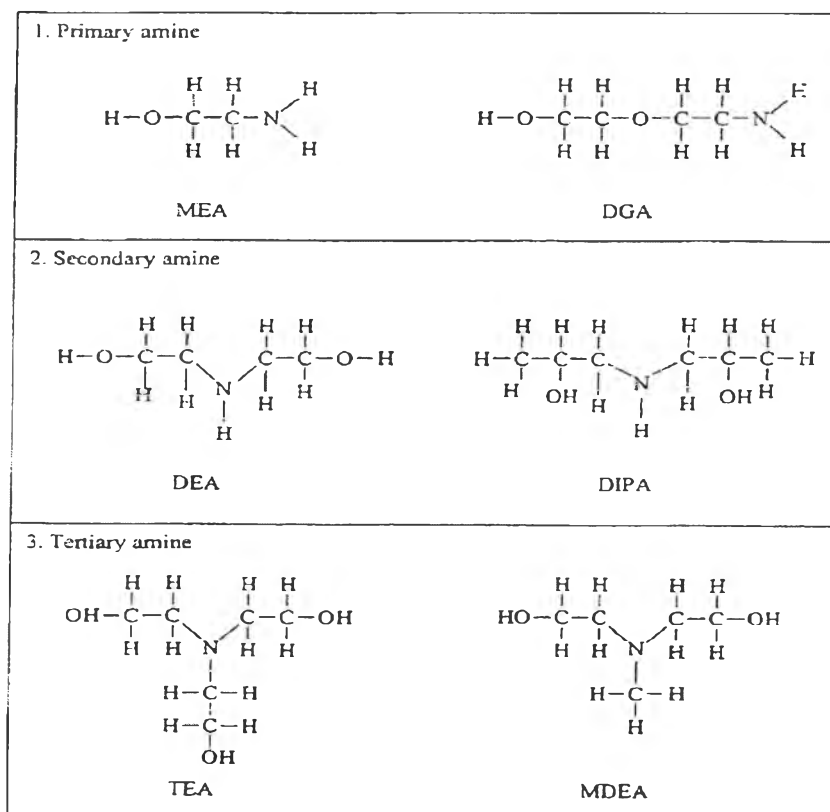
Table 2.2 Typical operating conditions and data for amines (Polasek and Bullin, 2006)

Amine:	MEA	DEA	DGA	MDEA
Solution strength, wt %	15-20	25-35	50-70	20-50
Acid gas loading, mole/mole (carbon steel)	0.3-0.35	0.3-0.35	0.3-0.35	Unlimited
Ability to selectivity absorb H_2S	No	Under Limited Conditions	No	Under Most Conditions

The MEA process is uneconomic for CO_2 capture from flue gas, as it requires high energy consumption to high temperature regeneration, high equipment corrosion rate, low CO_2 loading capacity, amine degradation by SO_2, NO_2, HCl, HF and oxygen in flue gas. Thus it requires making up MEA solution at high absorbent rate (Yang *et al.*, 2008). Alternatively, less reactive alknolamines, such as diethanolamine (DEA) and methyl diethanolamine (MDEA) are often used as absorbants (Gray *et al.*, 2005). The proposed mechanism of reaction between CO_2 and amines are shown in Figure 2.1.
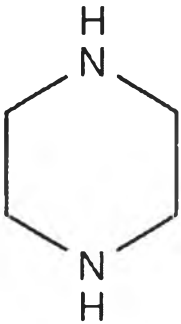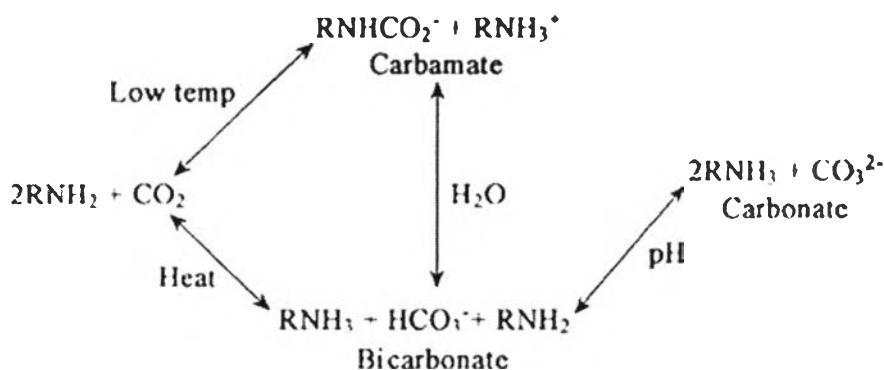

Figure 2.1 Proposed reaction sequence for the capture of carbon dioxide by liquid amine-based systems (Gray *et al.*, 2005).

2.3.2 Piperazine absorption technology

Piperazine (PZ) or diethylenediamine is an organic compound with six-membered ring consisting of two amine groups in its structure, called diamine as shown in Table 2.3. Piperazine is named after the 6-membered cyclic compounds with two nitrogens in the ring to be an azine. PZ is the corresponding azine of piperadine and it is usually manufactured by reacting of 1,2-dichloroethane with alcoholic ammonia.

Table 2.3 Chemical data and structure of piperazine (Sigma-Aldrich, 2012)

	Molecular formula	$C_4H_{10}N_2$
H N ⟨ ⟩ N H	Molar mass	86.14 g/mol
	Appearance	Solid
	Melting point	109-112 °C
	Boiling point	145-146 °C
	Solubility in water	0.9 g/L at 20 °C
	Acidity (pKa)	9.73*

* (Cullinane and Rochelle, 2006)

Previously, piperazine has been studied as a promoter for amine systems to improve kinetics. PZ has been investigated as a solvent and solvent-blend for absorption/stripping process for CO_2 capture in flue gas from coal-fired power plants. In addition, piperazine can be blended with different alkanolamine, such as MDEA/PZ or MEA/PZ because of its resistance to thermal and oxidative degradation at typical absorption/stripping conditions. The concentration of PZ when used as a promoter is low, between 0.5 and 2.5 m PZ, because PZ is not highly soluble. Given the nature and magnitude of absorption/stripping systems, any possibility of

precipitation ruled out PZ for use at concentrations above its room temperature solubility (Freeman *et al.*, 2009).

Cullinane and Rochelle (2006) compared overall rate constants of several amines at 1.0 M and 25 °C as shown in Table 2.4. Piperazine has the highest rate constant because of its structure and it may be attributed to the moderately high pKa. The cyclic diamine structure yields faster rates than would be expected from simple chemical classification or pKa correlation, as it can be observed from other diamine such as ethylenediamine (EDA) and heterocycles such as piperidine and morphorine.

Samanta *et al.* (2008) experimented on the absorption of CO_2 into PZ activated aqueous 2-amino-2-methyl-1-propanol (AMP) solutions at various temperatures with different relative compositions of AMP/PZ in the solutions and various CO_2 partial pressures. PZ acts as a rate accelerator in addition to combining with the advantage of high CO_2 loading capacity of AMP and relatively lower regeneration energy requirement. The solubility and diffusivity of CO_2 in the aqueous amine and activated amine solution containing 30 wt % total amine and with PZ concentrations of 2, 5 and 8 wt % were estimated in temperature range of 298-313 K using the N_2O- analogy method. The system was controlled in a wetted wall contactor with CO_2 partial pressure range of 2-14 kPa. It has been illustrated that adding a small amount of PZ to an aqueous solution of AMP enhance the rate of absorption of CO_2 and enhancement factor.

Freeman *et al.* (2009) studied on carbon dioxide capture with concentrated aqueous piperazine and the results have shown that PZ improved the solvent performance in absorption/stripping systems for CO_2 capture. For 8 m PZ, a CO_2 loading of approximately 0.25 mol CO_2/mol alkalinity was required to maintain a liquid solution without precipitation at room temperature (20 °C) with solubility of 14 wt % PZ, or 1.9 m PZ. The oxidative degradation of the concentrated PZ has shown to be four times slower than 7 m MEA in the presence of the combination with Fe^{2+}, Cr^{3+}, Ni^{2+} and V^{4+}. Also, the kinetic measurement have revealed that the rate of CO_2 absorption into 8 m PZ is more than twice that of 7 m MEA at 40 °C and nearly double at 60 °C.

Table 2.4 Overall rate constants for 1.0 M amine at 25 °C (Cullinane and Rochelle, 2006)

Amine	pKa	Rate constant $(s^{-1} \times 10^3)$	$\triangle Ha$ (kJ/mol)	Source (rate/pKa) Reference (Cullinane and Rochelle, 2006)
Piperazine	9.73	102.2	35.0	Cullinane and Rochelle, 2006
Monoethanolamine	9.55	5.9	41.2	Hikita *et al.*, 1997 : Perrin *et al.*, 1981
Diethanolamine	8.88	1.3	53.1	Hikita *et al.*, 1977 ; Christensen *et al.*, 1969
Diglycolamine	9.46	4.52	39.4	Alper *et al.*, 1990 ; Littel *et al.*, 1990
		6.7	40.1	Al-Juaied *et al.*, 2004: Littel *et al.*, 1990
Ethylenediamine	9.91	15.1		Jensen *et al.*, 1995; Christensen *et al.*, 1969
Piperidine	11.12	93.3		Sharma *et al.*, 1969; Christensen *et al.*, 1969
		60.3		Jensen *et al.*, 1952; Christensen *et al.*, 1969
Morpholine	8.94	20.6		Alper *et al.*, 1990 ; Christensen *et al.*, 1969
		20.0		Sharma *et al.*, 1965; Christensen *et al.*, 1969
		22.3	23.3	Al-Juaied *et al.*, 2004; Christensen *et al.*, 1969

Bougie *et al.* (2009) also worked on the kinetics of the reaction between CO_2 and piperazine-activated aqueous solution of a sterically hindered alkanolamine, 2-amino-2-hydroxymethyl-1,3propanediol (AHPD) in a wetted wall column contactor at 303.15 K, 313.15 K and 323.15 K. Increase of a small quantity of PZ increases the enhancement effect, while increasing the temperature will decrease the enhancement effect as shown in Figure 2.2. The reason for this was due to the latter tendency as

the activation energy of the second-order rate constant of AHPD, k_2 (53.7 kJ mol^{-1}; Bougie and Iliuta, 2009) was higher than the activation energy of the second-order rate of PZ, k_{2PZ} (30.8 kJ mol^{-1}).
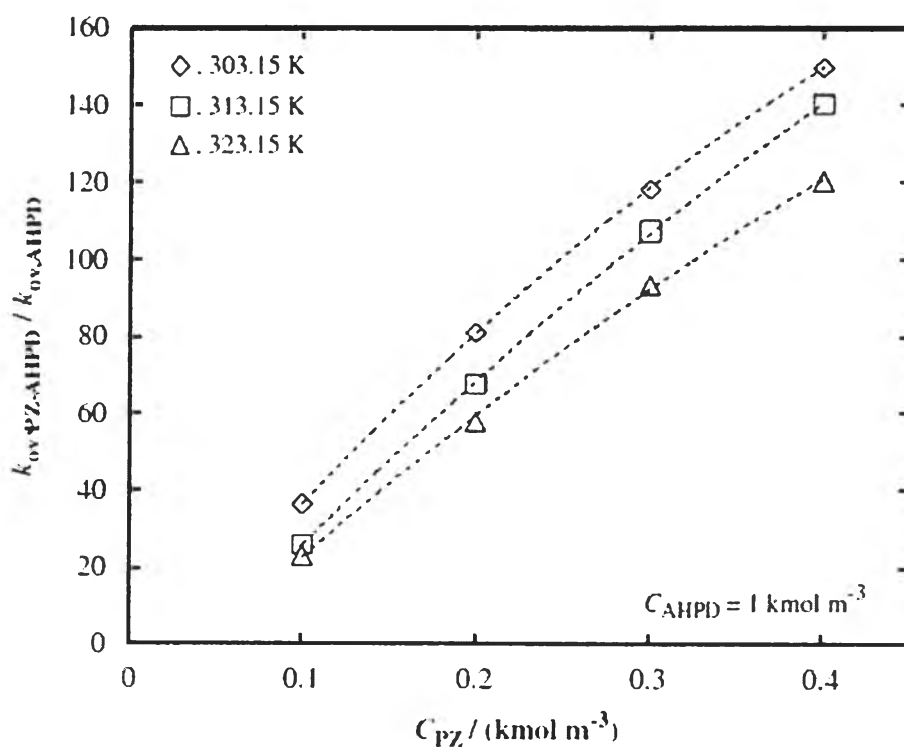

Figure 2.2 Enhancement effect of PZ in 1 kmol m^{-3} AHPD solution (Bougie *et al.*, 2009).

Rochelle *et al.* (2010) calculated a regressed electrolyte/NRTL model of 5 m piperazine at 40 °C as shown in Figure 2.3. At low loading, CO_2 reacts with piperazine to produce PZ carbamate and protonated PZ. The operation range was conducted at 0.31-0.41 gmol CO_2/equiv PZ, CO_2 reacted to produce protonated PZ carbamate and PZ dicarbamate.
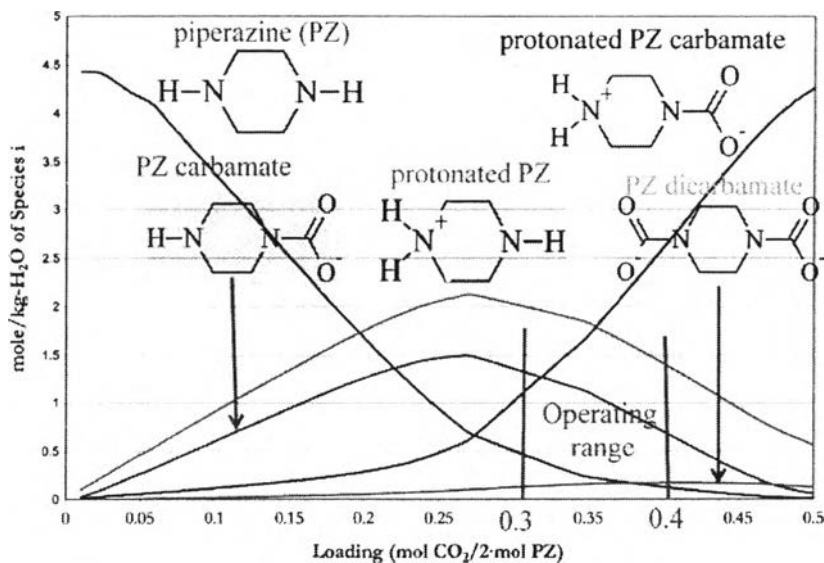

Figure 2.3 Speciation of 5 m PZ at 40 °C (Hilliard *et al.*, 2010).

2.3.3 Adsorption process technology

Adsorption is considered as one of the potential optional options because of the low energy requirement, cost advantage, and ease of applicability over a relatively wide range of temperatures and pressure. Besides, the success of this approach is dependent on the development of easily regenerable and durable adsorbent with a high CO_2 selectivity and adsorption capacity (Shafeeyan *et al.*, 2010). Adsorbent in term of supported amines have several advantages over liquid amines: (a) solvent loss due to evaporation can be less of an issue for supported amines compared to amine solutions and (b) vessel corrosion is less problematic with supported amines than liquid amines are used (Yan *et al.*, 2011).

The adsorption processes for gas separation via selective adsorption on solid media are also well known. These adsorbents can be operated via weak physisorption process or strong chemisorption interactions. Solid adsorbents are typically employed in cyclic, multi-module processes of adsorption and desorption, which desorption induced by two main adsorption technologies are being considered: pressure swing adsorption (PSA) and temperature swing adsorption (TSA). The difference between both technologies lies in the strategy to regenerate the adsorption after the adsorption step. In PSA applications, the pressure of the bed is reduced, whereas in TSA, the temperature is raised while pressure is maintained approximately constant (Plaza *et al.*, 2010). There are many types of solid adsorbent

used for gas separation, such as zeolites, activated carbon, mesoporous supports and metal-organic frameworks.

2.3.3.1 Types of physisorbent

2.3.3.1.1 Zeolite structural characteristic and CO_2 adsorption capacity (Chemsuschem, 2009)

Zeolite, a group of porous crystalline aluminosilicates built of a periodic array of TO_4 tetrahedra (T=Si or Al), have been widely used in separation applications mainly because of their unique ability of molecular sieving. The presence of aluminum atoms in these silicate-based molecular sieve materials introduces negative framework charges that are compensated with exchangeable cations in the pore space (alkali cations), and these structural characteristic of zeolites enable them to adsorb wide variety of gas molecules, including acidic gas molecules. The CO_2 adsorption properties of zeolites are also influenced by the porous characteristics of the framework. In comparison, on a number of commercially available zeolites including 4A, 5A, 13X, APG-II, and WE-G 592 that were being studied. It was reported that the highest adsorption capacities was observed in zeolite 13X, having the largest pore diameter and volume with a surface area of approximately 790 m^2/g (1995 Elsevier Science B.V).

2.3.3.1.2 Activated carbon structural characteristic and CO_2 adsorption capacity (Chemsuschem, 2009)

Activated carbons (AC) are well-known for adsorbent materials for many gas separations. These meso- or microporous carbonaceous structures have an advantage over other adsorbents due to their relatively low cost raw materials. AC can be produced from coals (e.g., bituminous coal, lignite) from industrial byproducts, (e.g., scraps of polymeric materials, petroleum, coke pitch), and wood or other biomass sources (e.g., saw dust, coconut shells, olive stones). Activated carbon can be prepared from raw materials consisting two steps: carbonization and activation. According to their large variations in the textural properties of activated carbons, such as pore size distribution, pore structure and active surface area, making

the adsorption characteristics highly variable (Sircar *et al.*, 1996). A gram of activated carbon can have a surface area in excess of 500 m^2, which 1500 m^2 can be readily reachable.

2.3.3.1.3 Mesoporous silica structural characteristic and CO_2 adsorption capacity

Mesoporous silica is a form of silica and a recent development in nanotechnology. The most common type of mesoporous nanoparticles are MCM-41 (Mobil Composition of Matter No.41) and SBA-15 mesoporous silica with pore size between 2-50nm. Since mesoporous silica has uniform and large pore size as well as high surface area, a large number of active sites or adsorption sites can be introduced uniformly on pore walls of mesoporous silica by its surface modification with organosilane molecules (Pankaj *et al.*, 2011). SBA-15 has a surface area in a range of 400-900 m^2/g (Beilstein, 2011) whereas MCM-41 has a surface area of 600-1000 m^2/g (Meziani *et al.*, 1997). However, the high cost of regeneration process, regenerable solid adsorbents appears to an option for CO_2 adsorption over the conventional method.

2.3.3.1.4 Biopolymer structural characteristic and CO_2 adsorption capacity

Chitosan (CTS) (hetero polymer constituted of glucosamine and a fraction of acetylglucosamine residues) is a well-known biopolymer characterized by its sorption properties due to its high nitrogen content (Krishnapriya *et al.*, 2010). They have become interesting not only because they are made from an abundant renewable resource, but because they are very compatible and effective biomaterials that are used in many applications. Chitosan is a linear copolymer of β-(1–4) linked 2-acetamido-2-deoxy-d-glucopyranose and 2- amino-2-deoxy-d-glycopyranose (Dash *et al.*, 2011).

Plaza *et al.* (2007) studies the CO_2 capture by adsorption with nitrogen enriched carbons. Different alkylamines (DETA, PEHA and PEI) were evaluated as a potential source of basic sites for CO_2 capture, and a commercial activated carbon

was used as a preliminary support in order to study the effect of the impregnation. The effect of the impregnation on the chemical properties of the carbon surface was studied by measuring the pH_{PZC} of the samples. The surface of the carbon changed from acidic (pH_{PZC} of 3.9), in accordance with the manufacturing process of the carbon, to basic (pH_{PZC} of around 9) after impregnation with strongly basic amines. The result of impregnation produces a dramatic decrease in the surface area due to the blockage of the pores. The sorbent performance in the capture of CO_2 was monitored by the mass increase of the sample when exposed to CO_2, and the capture capacity expressed as weight percentage of the fresh sorbent. In all cases, the highest capacity occurs at room temperature, the increase in temperature responds to the detriment of capture due to the exothermic character of physisorption for the activated carbon, and also to the contribution of the exothermic CO_2 sorption reaction in the case of the impregnated samples. The fact that the pure activated carbon presents the highest CO_2 capture capacity at room temperature is due to the higher contribution of physisorption, which is limited in the case of the modified sorbents due to the pores being blocked by the amine film. However, at medium temperature (70-90 °C), the contribution of chemisorptions associated to the incorporated amino group may improve the performance of the carbon.

Maroto-Valer *et al.* (2008) studied sorbents for CO_2 capture from high carbon fly ashes. The samples were steam activated at 850 °C, resulting in a significant increase of the surface area (1075 m^2/g). The activated samples were impregnated with different amine compounds methyldiethanolamine (MDEA), diethanolamine (DEA), monoethanolamine (MEA) and MDEA + MEA (MM) and the resultant samples were tested for CO_2 capture at different temperatures. The impregnation process with MDEA, DEA, MEA, and MDEA + MEA results in a decrease of the micro and mesopore volumes, resulting from pore filling effects. The mechanism of pore filling using different amine is not well understood, but it is assumed that the different pore filling effect was due to the difference in the molecular size and shape of the amines used. The highest adsorption capacity were at 30 and 70 °C for the amine impregnated activated carbons probably due to the combination of physical

adsorption inherent from the parent sample and chemical adsorption of the loaded amine groups.

Chang *et al.* (2009) prepared the CO_2 adsorption of mesoporous silicas including MCM-41(Mobil Composition of Matter No.41), SBA-15 mesoporous silica, and pore-expanded MCM-41 with pore size in the range of 2-17 nm, modified with mono-, di-, and tri-aminosilanes being examined in the study. The monoamine-loaded mesoporous silica denoted as 1N/MCM-41, 1N/SBA-15, and 1N/PE-SBA-15. The calcined mesoporous silica SBA-15 was functionalized by reacting with three primary and secondary aminosilanes, i.e. 3-aminopropyltriethoxysilane (APS), N-(2-aminoethyl)-3-aminopropyltrimethoxysilane (AEAPS), and (3-trimethoxysilylpropyl)diethylenetriamine (TA) under two grafting methods to give mono- (1N), di- (2N) and tri-amine (3N) grafted SBA-15s. The adsorption of the grafted amine under anhydrous CO_2 can be considered to proceed through carbamate intermediate and zwitterions mechanism as shown in Figure 2.4. The CO_2 adsorption capacity showed that SBA-15 was a better support than MCM-41 and pore-expanded SBA-15. The tri-amine-grafted SBA-15 exhibited a CO_2 adsorption capacity as high as 2.41 mmol/g under anhydrous CO_2 flow and 2.72 mmol/g under a CO_2 flow with relative humidity (RH) of 78 % at 333 K. When the CO_2 content in gas stream was varied, the result showed that the more CO_2 could be adsorbed as the partial pressure of CO_2 increased and lowered temperature.
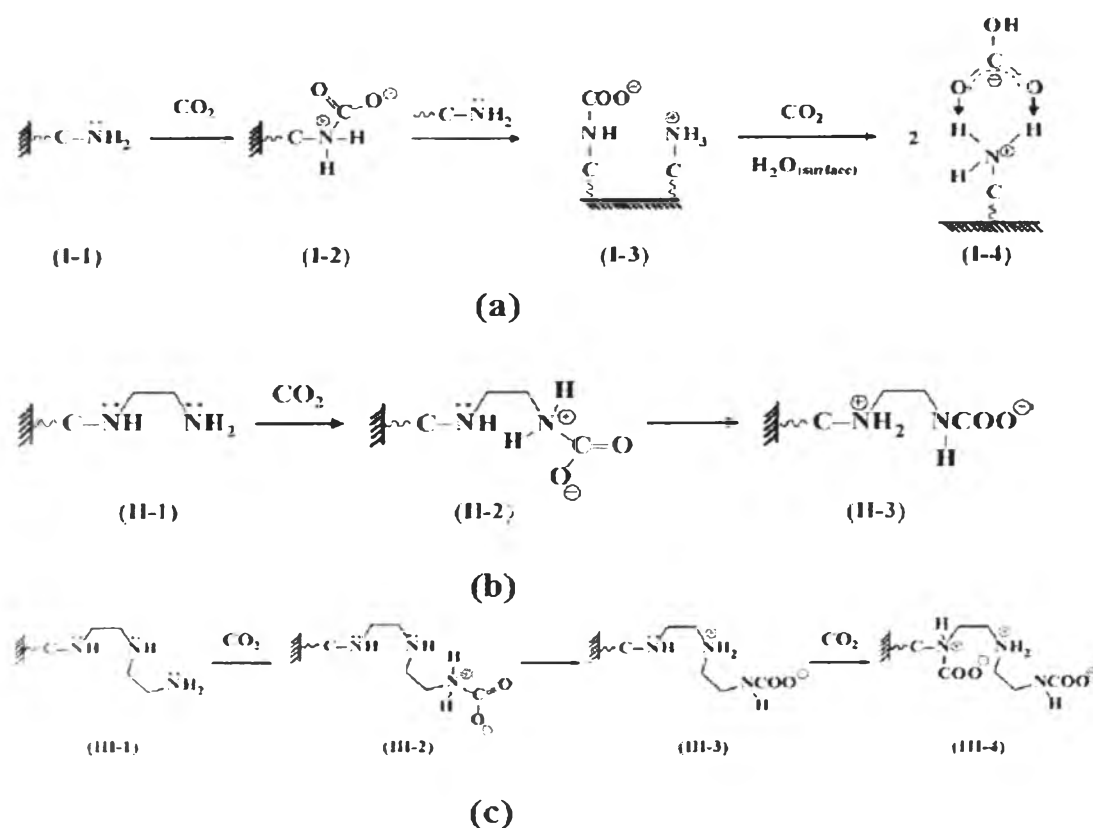
Figure 2.4 CO_2 reaction pathway with (a) monoamine- (b) di-amine- and (c) tri-amine-grafted on mesoporous silica (Chang *et al.*, 2009).

Chatti *et al.* (2009) tried to synthesize novel adsorbents by immobilization of different primary and secondary amine namely monoethanolamine (MEA), ethylenediaminee (ED) and isopropanol (IPA) on zeolite 13X matrix. Different paths of immobilization of amines in zeolite matrix were taken in aqueous media, organic media and through reflux method. The immobilization was expected to impart high adsorption capacity for CO_2 as compared to the bare zeolite 13X matrix. The maximum loading was achieved for methanol-mediated synthesis conducted using previously wetted pellets at room temperature and with 15mins of shaking time. In addition, the BET surface area and pore volume of zeolite 13X after the incorporation of MEA was observed which indicates that the amine molecules have occupied the pore volume due to the pore filling effect of MEA and surely that MEA was immobilized in the zeolite pores. The results were confirmed by using titrimetric analysis, gas chromatography (GC) with flame ionization detector (FID) and total organic carbon estimation (TOC). The CO_2 adsorption data from the breakthrough curve shows that the adsorption capacity of the amine loaded zeolite is increased approximately 20-30% in comparison with the bare zeolite matrix at 75 °C. Physico-

chemisorption was used to explain the adsorption. At ambient temperature, the physisorption is dominant over the chemisorption. However, at elevated temperature (75 °C), chemisorption is the dominant process due to the incorporation of the amine group in zeolite by means that at higher temperature adsorption capacity increases from the increasing of chemsisorption process.

Sanz *et al.* (2010) studied the pure CO_2 on SBA-15 impregnated with different amounts of branched polyethleneimine PEI (10, 30, 50 and 70 wt %). The temperature effect on adsorption was also studied in the range 25-75 °C showing that temperature strongly influenced CO_2 adsorption capacity. The powder XRD patterns of PEI-impregnated samples demonstrate the same diffraction peaks, despite that their intensities gradually decrease as the amount of PEI-loaded is increased as shown in Figure 2.5. It is indictable that for the highest amount of PEI-loaded (50 and 70%), it was probably due to the partial filling of pores. The maximum amount of PEI organic polymer that could fill the SBA-15 pores (pore volume of $1.10 cm^3$) will be 1.155g, which corresponds to a 53.6% of PEI in the sample. Thus, for SBA-15-PEI (70), PEI is not only occupying the porosity of the silica, but 17.8% of added PEI is necessarily surrounding silica particles. On the other hand, the effect of temperature on the adsorption process was studied by running adsorption experiments at 25, 45 and 75 °C with SBA-15-PEI (50). A large difference was found in adsorption capacity at 1 bar that changed from 36.7 to 75.0 mg/g when increasing temperature from 25 to 45 °C. With the PEI loadings around 50-70%, the adsorption capacity at 1 bar is almost the maximum capacity achievable for these two loadings, even higher than adsorption capacity of SBA-15 at the highest pressure studied close to 6 bars. The observed temperature dependence cannot be explained in terms of thermodynamic but considering kinetic effects. Increasing the temperature promotes a higher mobility, increases in the kinetics of access of CO_2 to the regions that are not easily accessible at lower temperatures.
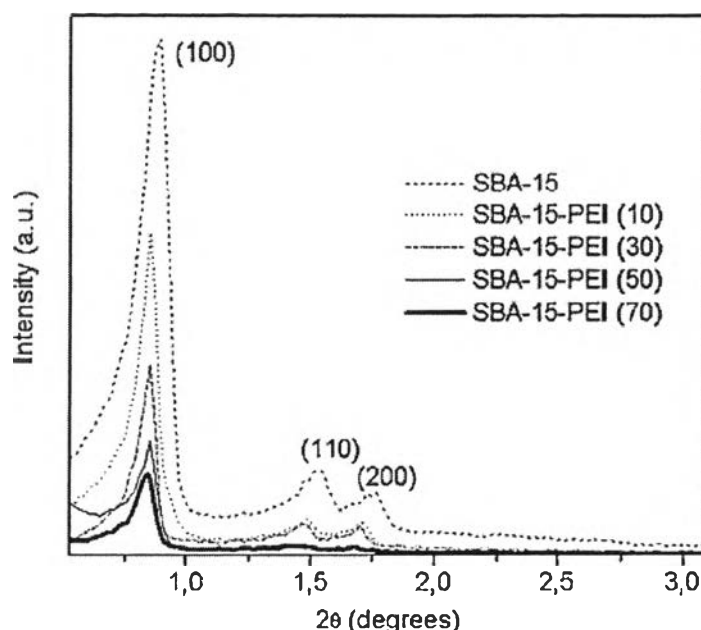
Figure 2.5 Powder XRD patterns of pure SBA-15 and functionalized samples SBA-15-PEI(x) (Sanz *et al.*, 2010).

Sharma *et al.* (2011) investigate the information on CO_2 adsorption, three types of mesoporous materials, MCM-41, MCM 48 and SBA-15 were synthesized, pelletized and further pellets were impregnated with 50 wt % of polyethyleneimine (PEI) in methanol to determine the performance of the material in terms of CO_2 adsorption. The CO_2 adsorption/desorption performance of the materials was performed on a homemade fixed bed reactor at different temperature (40, 60 and 80 °C) and pressure at 0 to 1 atm. The materials were characterized by XRD, TGA, FT-IR, SEM, TEM, N_2-physisorption and BET techniques. The powdered mesoporous materials were shaped into pellet type adsorbent. Different binders, activated carbon, calcium sulfite ($CaSO_3$), calcium titanate ($CaTiO_3$) were added to induce additional changes in its property. After PEI impregnation, there is decrease in surface area, pore volume and pore diameter but N_2 adsorption-desorption study again proved that the value of surface area, pore volume and average pore diameter of MCM-48 are greater than MCM-41 and SBA-15 and all these combined feature enable MCM-48 to be better accommodate the bulky PEI with little hindrance and allow higher loading inside channels as compared to MCM-41 and SBA-15. This is also supported by a higher mechanical strength of MCM-48 pellet.

Sayari *et al.* (2011) reviews adsorbents used for flue gas treatment via CO_2 adsorption with a) physical adsorbents including carbons, zeolites and metal organic

frameworks (MOFs) and b) chemical adsorbents, amine-functionalized materials with the aim of developing suitable CO_2 adsorbents. Suitable adsorbents for CO_2 removal from flue gas implies of combining several attributes, including i) high CO_2 adsorption capacity, ii) fast kinetics, iii) high CO_2 selectivity, iv) mild condition for regeneration, v) stability during extensive adsorption, vi) tolerance to the presence of moisture and other impurities in the feed, vii) low cost. As a result, at low CO_2 partial pressure, activated carbons exhibits lower adsorption capacity and selectivity than zeolites due mainly to their less favorable adsorption isotherms. In spite of the hydrophobic character of carbon-based adsorbents, their CO_2 adsorption ability is adversely affected by the presence of water vapor. Zeolites and zeolite-like materials with low Si/Al ratios are among the most promising adsorbents for CO_2 capture from flue gas but needs extensive drying prior to capture CO_2. Metal organic frameworks (MOFs), zeolite-like MOFs ZMOFs and covalent organic frameworks (COFs) may be promising material for CO_2 removal provided that more favorable CO_2 adsorption isotherms obtained but their selectivity and capacity at low pressure of CO_2 in gas mixtures are quite low and more likely to be suitable for CO_2 storage rather than CO_2 separation from flue gas. Apart from the physical adsorbents, the selectivity of amine-functionalized materials is not significantly affected by temperature within the range of flue gas treatment. In addition, their stability may be dramatically enhanced during thousands of adsorption-desorption cycles providing that the feed and purge gases contain moisture. Summary of the CO_2 adsorption capacity from literature review with different types of adsorbents are shown in Tables 2.5 -2.9.

Table 2.5 Literature review of CO_2 adsorption properties of activated carbons and carbon nanotubes at low pressure (Sayari *et al.*, 2011)

Carbon material	Temperature (K)	CO_2 adsorption capacity at 0.1-0.4 bar (mmol/g)	N_2 adsorption capacity at 0.9-1.6 bar (mmol/g)	CO_2/N_2 capacity molar ratio	Reference Sayari *et al.*, 2011
AC	298	0.6-1.5	0.5-0.75	1.2-2	Na *et al.* (2001)
AC	328	0.25-0.8	0.2-0.35	1.25-2.28	Na *et al.* (2001)
SWCNT	308	0.5-1.25	-	-	Cinke *et al.* (2003)
MWCNT	333	0.34-0.91	-	-	Su *et al.* (2009)

Table 2.6 Literature review of CO_2 adsorption properties of some zeolites and zeolite-like materials at low pressure (Sayari *et al.*, 2011)

Zeolite/Si/Al ratio	CO_2 adsorption temperature (K)	Adsorption capacity at 0.1-0.4 bar (mmol/g)	N_2 adsorption capacity at 0.9-1.6 bar (mmol/g)	CO_2/N_2 capacity molar raito	Reference Sayari *et al.*, 2011
NaX/1	298	2.8-3.9	0.264-0.46	11-8.5	Cavinati *et al.* (2004)
NaX/1	323	1.43-2.49	-	-	Cavinati *et al.* (2004)
LiX/1	303	3.1-4.6	-	-	Walton *et al.* (2006)
NaY/2.4	323	0.45-1.17	-	-	Maurin *et al.* (2007)
CsY/2.4	333	0.86-1.2	-	-	Pimgruber *et al.* (2010)
KY/2.4	333	0.75-1.6	-	-	Pimgruber *et al.* (2010)
Silicalite/∞	334	0.16-0.45	0.1	1.6	Dunne *et al.* (1996)
H-ZSM-5/30	313	0.7-1.5	0.23	3	Harlick *et al.* (2002)
Li-MCM-22/15	333	0.68-1	-	-	Zukal *et al.* (2009)

Table 2.7 Literature review of CO_2 adsorption properties of some MOFs and ZMOFs (Sayari *et al.*, 2011)

MOFs	Temperature (K)	CO_2 adsorption capacity (mmol/g at 0.1-0.4 bar)	N_2 adsorption capacity (mmol/g at 0.9-1.6 bar)	CO_2/N_2 selectivity	Reference Sayari *et al.*, 2011
MOF-508	323	0.1-0.7	0.6-0.9	2	Bastin *et al.* (2008)
Cu-BTC	298	0.5-2	0.25	15	Yang *et al.* (2007)
MIL-53	303	0.5-1.15	-	-	Finsy *et al.* (2009)
Ni/DOBDC	296	2.7-4.01	-	-	Caskey *et al.* (2008)
CO/BOBDC	296	2.8-5.36	-	-	Caskey *et al.* (2008)
Mg/DOBDC (Mg-MOF-74)	296	5.36-6.8	-	-	Britt *et al.* (2009)
ZIF-78	298	0.77-1.36	-	50	Banerjee *et al.* (2009)

Table 2.8 Literature data on CO_2 adsorption capacity of amine-impregnated adsorbent (Sayari *et al.*, 2011)

Support	Amine	Amine loading (wt %)	CO_2 adsorption capacity (mmol/g)	CO_2/N	Experimental condition		Reference Sayari *et al.*, 2011
					CO_2 concentration (%)	T (°C)	
MCM-41	PEI	50	2.1	0.18	10	75	Xu *et al.* (2002)
MCM-41	PEI	50	2.84	0.27	13(13% H_2O)	75	Xu *et al.* (2005)
SBA-15	PEI	50	3.18	0.27	15	75	Ma *et al.* (2009)
KIT-6	PEI	50	1.95	0.17	5	75	Son *et al.* (2008)
Monolith	PEI	65	3.75	0.25	5	75	Chen *et al.* (2009)
As-synthesized SBA-15	TEPA	50	3.25	0.28	10	75	Yue *et al.* (2006)
As-synthesized MCM-41	TEPA	50	4.54	0.34	5	75	Yue *et al.* (2008)
As-synthesized SBA-15	TEPA+DEA	50(30% TEPA,20% DEA)	3.77	0.38	5	75	Yue *et al.* (2008)
PE-MCM-41	DEA	76	3	0.41	5	25	Franchi *et al.* (2005)
Mesoporous Al_2O_3	DETA	40	1.4	0.12	100	57	Plaza *et al.* (2008)
Mesoporous SiO_2	PEI	40	2.4	0.26	15	70	Sayari *et al.* (2010)
SBA-15	PEI	50	1.36	0.12	12	75	Dasgupta *et al.* (2009)
PMMA	TEPA	41	13.88	1.28	15 (2.6% H_2O)	70	Lee *et al.* (2008)
PMMA	Ethyleneamine + acrylonitrile	Proprietary information	4.18	Proprietary information	10 (humid)	25	Gray *et al.* (2005)
PMMA	DBU	30	2.34	0.59	10 (2% H_2O)	65	Gray *et al.* (2008)
SiO_2 (CARiACT)	PEI	40	3.95	0.42	10 (2% H_2O)	40	Jadhav *et al.* (2007)
PMMA (Diaion)	PEI	40	3.60	0.39	10 (2% H_2O)	40	Gray *et al.* (2009)
AOS carbon	PEI	5	1.98	1.70	100	25	Plaza *et al.* (2009)
13X	MEA	25	0.45	0.11	15	75	Jadhav *et al.* (2007)

Beta-zeolite	TEPA	38	2.08	0.21	10	30	Fisher *et al.* (2009)

Table 2.9 Literature data on CO_2 adsorption of amine-grafted adsorbent (Sayari *et al.*, 2011)

Support	Amine	CO_2 adsorption capacity (mmol/g)	Amine loading (mmol/g)	CO_2/N	Experimental conditions		Reference Sayari *et al.*, 2011
					CO_2 concentration	T (° C)	
Silica gel	AP	0.89	1.26	0.71	100% (100% RH)	50	Leal *et al.* (1995)
MCM-48	AP	2.3	2.3	1	10% (100% RH)	25	Huang *et al.* (2003)
HMS	AP	1.59	2.29	0.69	90%	20	Knowles *et al.* (2006)
HMS	TRI	1.34	4.57	0.29	90%	20	Knowles *et al.* (2006)
PE-MCM-41	TRI	1.59	7.9	0.20	10%	50	Serna-Guerrero *et al.* (2010)
SBA-15	TRI	1.80	5.80	0.31	15% (humid)	60	Hiyoshi *et al.* (2005)
MS	TRI (co-cond)	1.74	5.18	0.34	100%	25	Kim *et al.* (2008)
SBA-16	EDA	1.4	0.76	1.84	100%	27	Knofel *et al.* (2007)
SBA-15	AP	0.45	2.56	0.18	10%	65	Wang *et al.* (2007)
SBA-16	EDA	0.727	3.06	0.24	15%	60	Wei *et al.* (2008)
SBA-15	AP	1.54	2.72	0.57	10%	25	Zelenak *et al.* (2008)
SBA-12	AP	1.04	2.13	0.49	10%	25	Zelenak *et al.* (2008)
MS	AP	0.24	1.6	0.15	10%	30	Knofel *et al.* (2009)
MSP	EDA	0.73	0.99	0.73	10%	60	Lu *et al.* (2009)
MCM-48	TREN	1.36	4	0.34	100%	50	Bhagiyalakshmi *et al.* (2010)
ITQ-6	AP	0.67	1.26	0.53	12%	20	Zukal *et al.* (2009)
SBA-15	Amine-dendrimers	1	1.25	0.40	90%	20	Liang *et al.* (2008)
SBA-15	Aziridine polymer	4	9.78	0.41	10% (humid)	75	Drese *et al.* (2009)